# Cardiac Resynchronization by Cardiosphere-Derived Stem Cell Transplantation in an Experimental Model of Myocardial Infarction

**Michael Bonios, MD**, **Connie Y Chang, MSE**, **Aurelio Pinheiro, MD**, **Veronica Lea Dimaano, MD**, **Takahiro Higuchi, MD, PhD**, **Christina Melexopoulou, MD**, **Frank Bengel, MD**, **John Terrovitis, MD**, **Theodore P Abraham, MD**, and **M. Roselle Abraham, MD**
Johns Hopkins University, Baltimore, MD

## Abstract

**Background**—Cardiosphere-derived cell (CDC) transplantation can improve global left ventricle ejection fraction (LVEF) post-infarction (MI). Here, we examined the effects of CDC transplantation on regional function and dyssynchrony post-MI.

**Methods**—Two million rat CDCs(n=7) or saline(PBS;n=7) were injected into the infarct region of WK rats. Infarct size and CDC localization were evaluated by positron emission tomography (PET; n=7). Two dimensional and strain echocardiography were performed at 1&4 weeks post-MI. LVEF, circumferential strain and time to peak circumferential strain were measured in the basal and apical short axis views. Dyssynchrony was defined as max difference of time to peak circumferential strain of opposing segments in each short axis view. Engraftment was measured by quantitative polymerase chain reaction(PCR).

**Results**—PET revealed that infarct size was 15.4 ±3.6% of the LV and CDCs were localized to the infarct and border-zone. CDC transplantation improved LVEF (45±8 to 52±7%,p=0.02), mean circumferential strain (−7±2 to −10±1%,p=0.02) and dyssynchrony (45±10 to 28±11ms,p=0.04) of the infarct/peri-infarct zone from 1 to 4weeks post-MI, despite CDC engraftment of only 2.4±3%. In contrast, LVEF (48±5 to 40±4%,p=0.03) and mean circumferential strain (−8±2 to −7±1%, p=0.02) of the infarcted region deteriorated, with no significant change in dyssynchrony (42±12 vs. 46±13ms,p=0.6) in the PBS group during the same time period. Change in LVEF correlated with change in circumferential strain (r=−0.8,p=0.002) and dyssynchrony (r=0.6,p=0.02) of the infarct/peri-infarct region at 4weeks post-MI.

**Conclusion**—CDC therapy enhanced LVEF by improving circumferential strain and decreasing dyssynchrony of the infarct/peri-infarct region at 4 weeks, but not 1 week post-MI. Cellular resynchronization therapy (CRT) using CDCs may be an alternative to traditional electrical CRT in post-MI dyssynchrony.

**Address for correspondence:** M. Roselle. Abraham, MD 720 Rutland Ave, Ross 871 Johns Hopkins University, Baltimore, MD, USA, 21210 Phone: (410) 502-2685 FAX: (410) 502-2096 mabraha3@jhmi.edu.

**Publisher's Disclaimer:** This is a PDF file of an unedited manuscript that has been accepted for publication. As a service to our customers we are providing this early version of the manuscript. The manuscript will undergo copyediting, typesetting, and review of the resulting proof before it is published in its final citable form. Please note that during the production process errors may be discovered which could affect the content, and all legal disclaimers that apply to the journal pertain.

**Conflict of interest:** None

**Financial disclosure:** None

**Keywords**

Stem cells; dyssynchrony; strain; echocardiography; PET

## Introduction

Myocardial infarction is an important cause of heart failure.(1) Left ventricular dyssynchrony, frequently observed in heart failure is a predictor of poor outcome. Cardiac resynchronization therapy (CRT) can reduce symptoms, induce reverse remodeling and improve survival, but patients with ischemic cardiomyopathy often do not respond to this therapy.(2,3) Stem cell transplantation is a novel therapy that offers the potential of regenerating myocardium and improving mechanical synchrony post-infarction (MI). (4)

Autologous cardiosphere-derived stem cell (CDC) therapy is currently in phase 1 clinical trials in the U.S.(CADUCEUS, see www.clinical trials.org) Cardiosphere-derived cells (CDCs) are progenitor cells derived from monolayer outgrowth of heart tissue and are comprised of subpopulations of cells with markers of cardiac progenitor cells (c-kit$^+$/CD90$^-$), mesenchymal stem cells (c-kit$^-$/CD105$^+$,90$^+$) and endothelial cells (c-kit$^-$/CD34$^+$), that together, have a synergistic effect on cardiac regeneration.(5) Experimental studies reveal that upon transplantation into infarcted myocardium, CDCs secrete paracrine factors, differentiate into endothelial cells or cardiac myocytes (6),(7) and improve LVEF (5). Since paracrine factors can impact global cardiac function, it is essential to determine the contribution of improved regional function of the infarcted region to increase in LVEF following CDC transplantation post-MI. Here, we investigated the contribution of regional cardiac function and mechanical dyssynchrony in the recovery of LVEF post-CDC transplantation in a syngeneic rat model, since it permits cell tracking by PET, detailed assessment of cardiac function by echo and quantification of engraftment by quantitative PCR. We hypothesized that CDC therapy would improve function by inducing reverse remodeling of the infarcted region. Our results indicate that despite low levels of CDC engraftment, circumferential strain and dyssynchrony improved in the infarct/peri-infarct region, and were correlated with increase in LVEF 4wks post-MI.

## Methods

### Isolation of cardiosphere-derived stem cells and tissue culture

CDCs were isolated from hearts of male, 3 month old, Wistar Kyoto (WKY) rats (Harlan, Indianapolis, Indiana, USA) as described previously.(5,8) Briefly, small pieces of myocardial tissue (explants) derived from young male rats were placed on fibronectin coated dishes. In the following days, cells exited the explants and formed an adherent monolayer on the dish surface with phase bright cells on top. These cells are harvested with mild enzymatic digestion and transferred to D-poly-lysine coated dishes, where they form three dimensional structures called cardiospheres which are enriched in cardiac progenitors. Cardiospheres are subsequently harvested and grown as monolayers in fibronectin-coated flasks – these cells are called cardiosphere-derived cells (CDCs). CDCs were cultured in IMDM medium (containing 4.5 gm/l glucose, 20% FBS, 10% glutamine, 10% Pen/strep and 0.1mM mercaptoethanol) and expanded to 3 passages prior to transplantation.

### Animal surgery - cell injection

Rats were chosen for these studies because they permit detailed assessment of cardiac mechanics by echocardiography, cell tracking by in vivo PET and quantification of engraftment by PCR. We used WKY rats, which are genetically identical and performed

gender mis-matched transplantation: CDCs derived from male rats were injected into female rats, in order to permit quantification of engraftment by quantitative PCR, for the male-specific SRY gene.

Female WKY rats weighing 180-200gm were used. Animals were intubated; anesthesia was induced with 4% isoflurane inhalation and maintained with 2% inhalation. The heart was exposed through a left lateral thoracotomy, MI was induced by permanent ligation of the mid portion of the left anterior descending coronary artery (LAD) using a silk 5.0mm suture (Ethicon) and animals were randomly assigned to two groups, namely **PBS/control** (n=7) or **CELL** (n=7) **group**. Immediately following LAD occlusion, 100 uL of PBS or $2 \times 10^6$ rCDCs, suspended in 100uL of $Ca^{2+}$ and $Mg^{2+}$-free PBS were injected intra-myocardially into 2 sites of the infarct region, using a 28G needle, the chest was closed and animals were allowed to recover.

### PET imaging

In vivo PET imaging of $^{18}FDG$-labeled rCDCs and myocardial perfusion($^{13}NH_3$) were performed in a separate group of animals (n=7) to characterize the infarct model and examine CDC localization post-transplantation. Please see the supplemental data section for details of PET imaging and data analysis.

### Echocardiography

We performed echocardiograms in 10 non-infarcted rats, and in infarcted rats at 2 time points, namely, 1 and 4 weeks post-MI. We chose the 1 week time point because of poor image quality early after MI due to presence of a left-sided pneumothorax. Rats were anesthetized with 1.5% isoflurane (using a nose cone) for the duration of imaging; heart rate was monitored and the animals' body temperature was maintained at 37°C during image acquisition. We used a 14-MHz transducer coupled to a Vivid 7 echocardiography machine (GE Medical, Milwaukee, WI). Two dimensional long axis images were used for ejection fraction measurements (calculated as the difference between end-diastolic and end-systolic volumes normalized to end-diastolic volume, expressed as a percentage). Subsequently, an *apical short axis image* (distal to the papillary muscles, including the infarcted region) and *basal short axis image* (basal to the infarcted region, at the level of the papillary muscles) were acquired. Left ventricular ejection fraction was calculated using the area-length method.(9) The adjustments of the sector width for this transducer resulted in a maximum frame rate of 90-100 frames/sec.

**Circumferential strain—**Initially, we analyzed radial and circumferential strain for measurement of dyssynchrony. In the first 2 animals, we noted significant variability in peak amplitude of strain and time to peak strain in the radial direction. Hence, we restricted our analysis to circumferential strain. Additionally, circumferential strain has been shown to be a more dynamic parameter and indicative of dyssynchrony in an experimental model.(10) Furthermore, the feasibility and reproducibility of circumferential strain in small animals is superior to longitudinal and radial strain. Apical long axis views in rodents are challenging to obtain repeatedly, reducing the feasibility of longitudinal strain. Similarly, due to sampling issues, radial strain correlates poorly with reference standards and appears more variable in validation studies.(11) Circumferential and radial strain contribute to overall changes in chamber volume over the cardiac cycle more so than longitudinal strain and thus would better reflect changes in ejection fraction in our model.

Image processing was performed off-line. We used the speckle-tracking algorithm in the EchoPac SW 7.1.1 version PC workstation (GE Medical) in order to measure circumferential strain. Based on the 2D short axis images (SAX), the end-systole and end-

diastole time points were defined; subsequently, three different cardiac cycles from each acquisition were selected for further analysis. Briefly, after selecting the cardiac cycle, the software prompts the operator to apply a region of interest in a 'click to point approach' in order to delineate the endocardium. Subsequently the software automatically defines an epicardial and mid-myocardial line and processes all frames of the selected cardiac cycle. Then, the software automatically outlines 6 segments per short axis view. The circumferential strain value was calculated for each segment. Circumferential strain values are negative values; as contraction progresses, the circumferential strain values become more negative. Segments with poor quality tracking were excluded from the analysis. For the apical short axis views we identified the segment with the lowest circumferential strain value, at 1 and 4 weeks post-MI for each animal and refer to it as _regional strain of infarcted_ region. _Mean circumferential strain_ was defined as the average strain of all segments in a particular short- axis view. Intra-observer and inter-observer variability analyses were performed using five randomly selected studies. For intra-observer analysis, measurements of the five selected studies were repeated on 2 separate occasions by the same observer. Inter-observer analysis was performed by two independent observers who were blinded to the results of each other.

**Mechanical dyssynchrony evaluation—**In all animals and for all myocardial segments, the time to peak circumferential strain value was calculated using GE analysis software. For each animal, mechanical dyssynchrony was assessed for the apical and basal SAX acquisitions at 1 and 4 weeks post-MI, by measuring inter-segmental mechanical delay. More specifically, the time delay between opposing myocardial segments of the basal and the apical SAX view was calculated separately and the higher measured delay was used as a measure of mechanical dyssynchrony for the base and apex respectively. Three different cardiac cycles were analyzed and the values were averaged.

## Real time quantitative polymerase chain reaction for quantification of engraftment (q-PCR for rat SRY gene)

Animals from the cell-injected group were sacrificed 4 weeks after CDC transplantation; hearts were explanted, weighed and homogenized. Injection of CDCs harvested from male rats into female recipients permitted use of the male-specific SRY gene, located on the Y chromosome, as a target for qPCR. (12) Since there is only one copy of the SRY gene per cell, the number of copies of the SRY gene (determined by qPCR) in the recipient heart corresponds to the number of transplanted cells. (See supplemental methods)

## Statistics

Values are reported as mean ± SD. The paired *t*-test was used for intra-group comparisons of the echocardiography measurements at 1 and 4 weeks post-MI. The Spearman′s correlation coefficient was used to assess correlation of the echocardiography parameters. The independent sample *t*-test was used to compare the EF values of the 2 groups at 1 and 4 weeks post-MI. A p value less than 0.05 was considered statistically significant. Mean difference, standard error, upper and lower 95% confidence interval limits and *t* tests were performed for calculation of inter-observer and intra-observer variability. (13)

# Results

## Characterization of infarct model by PET

Infarct size in this model was 15.4 ±3.6% of the LV. Intra-myocardial CDC injection resulted in cell localization in the infarct and border-zone (Figure 1).

### Non-infarcted, baseline echocardiography parameters

Baseline echo parameters were measured in non-infarcted rats (n=10) and are shown in table 1: Mean circumferential strain at the apex (n=9) and base (n=9) was similar. Mechanical delay of the base and apex was 12.1±5.6msec and 9.4±2.5msec respectively (p=NS).

### CDC transplantation improved LVEF post-MI

There was no significant difference in LVEF between the two groups of animals, one week post-MI (p=0.3), indicating that all animals suffered a similar ischemic insult. However, 4 weeks post-MI, there was a significant increase in LVEF in the CELL Group (44.6±7.6% vs 51.5±7.4%, p=0.02,) and a significant decrease in the PBS Group (47.8±4.8% vs 40.2±4.2%, p=0.02) (Figure 2A). Left ventricular end systolic (LVESV) and end diastolic volume (LVEDV) did not differ significantly among the PBS and CELL groups at 1 week post-MI (LVESV, 128±13 vs 133±28uL, & LVEDV, 248±24 vs 240±38uL, p=NS). At 1 month post-MI, LVESV was 227±64uL in the PBS group, (increased by 76.5%; p=0.011), and 183±80uL in the CELL group (increased by 37.6%; p=0.129). LVEDV was 386±111uL in the PBS group (increased by 55.8%; p=0.018) and 365±117uL in the CELL group (increased by 52.0%; p=0.033).

### Regional circumferential strain in infarct/peri-infarct region is increased by CDC transplantation

Intra-observer reproducibility was high for strain (mean difference 1%; 95% C.I. 1.0 to −1.0%). Similarly, no significant differences were noted in inter-observer measurements for strain (mean difference 1%; 95% C.I. 3.0 to −3.0%). We excluded 3.1% of the segments from analysis due to poor tracking quality.

There was no significant difference in circumferential strain between the CELL and PBS-treated groups at 1 week following transplantation. In the CELL group, from week 1 to week 4, there was a significant improvement (−7.3±1.8% to −10.4±1.3%, p=0.02) in mean apical circumferential strain. In contrast, in the PBS group, mean circumferential strain significantly worsened (−8.1±2.0% to −6.6±1.3%, p=0.02; Figure 2B). In the CELL group, the regional circumferential strain in the infarcted area improved significantly from week 1 to week 4 post-MI (−2.4±1.5% to −5.4±1.8%, p=0.01), but did not change in the PBS (−2.4±2.0% vs −2.2±1.2%, p=0.8) group (Figure 2C). Increase in LVEF in the CDC-treated animals correlated with improvement in mean circumferential strain of the apex (r= −0.78, p=0.002; Figure 2D) and regional strain of infarcted region (r= 0.7, p=0.005).

In both groups, mean *circumferential strain* measured in the *basal* short axis images (non-infarcted region) did not change significantly from week 1 to 4 post-MI (Figure 3A; from −19.0±2.9 to −17±2.4, p=0.398, PBS Group and from −19.4±2.2 to −20±1.5, p=0.416, CELL group) and was not correlated with change in global EF (r=−0.33, p=0.3; Figure 3B)

### Dyssynchrony in infarct/peri-infarct region is decreased by CDC transplantation

There was no significant difference in mechanical delay between the PBS and CELL-treated groups 1 week post-transplantation/MI (Figure 4C). Maximal mechanical delay (dyssynchrony) in the infarct/peri-infarct region (apex) decreased significantly from week 1 to week 4 post-MI in the CELL group (45.3±9.8 msec vs 28.37±11.1 msec, p=0.04) (Figure 4A) but there was no significant change in the PBS (42.4±12.0 msec vs 45.7±12.6 msec, p=0.6) (Figure 4B) group. Furthermore, no significant change in mechanical delay was observed during this time period in the basal short axis acquisitions (9.2±3.1 to 22.7±13.4msec; p=0.079 for the PBS Group and 7.5±2.5 to 11.6±4.8 msec; p=0.054 for the CELL group). In both groups and at all time points, the apical segments demonstrated

greater mechanical delay in comparison to the basal segments. Finally, decrease in dyssynchrony correlated with improvement of LVEF (r=0.6, p=0.02) (Figure 4D).

Heart rate did not differ significantly from week 1 to week 4 in the PBS (307±37 bpm vs 287±58 bpm, p=0.2) and CELL (277±22 bpm vs 277±19 bpm, p=0.9) groups.

### Low CDC engraftment at 4 weeks post-transplantation

Using quantitative PCR, we found that 2.4±3.3% or approximately 48,000 CDCs were present (engrafted) in the heart 1 month post-transplantation.

## Discussion

The main findings of this study are that CDC transplantation into ischemic myocardium improved LVEF by augmenting circumferential strain and decreasing dyssynchrony of the infarct/peri-infarct region, at 4 weeks (but not 1 week) post-MI/transplantation. Our results are concordant with previous cell therapy studies, wherecell transplantation post-MI improved left ventricular function and dyssynchrony.(4),(14) These studies examined the effects of transplanting human cells derived from the bone marrow (4) or cord blood on (14) strain/dyssynchrony following myocardial infarction via the intra-myocardial and intra-ventricular route respectively. Our study extends the findings of these two studies by quantifying strain (within, near and remote from the infarct), dyssynchrony and engraftment in a syngeneic small animal model of cardiac-derived stem cell transplantation acutely post-MI. Taken together, these 3 studies indicate that irrespective of the stem cell type, route and timing of cell transplantation (relative to MI), improvements in regional/global strain and dyssynchrony underlie functional improvement following cell therapy.

In post-MI models, infarct expansion and LV remodeling begin within hours after MI and progress,(15) resulting in worsening strain in the infarct and peri-infarct regions. (16) Here, we demonstrate significant improvements in LVEF in CDC-treated animals, but not PBS treated animals at 4 weeks post-MI, which is similar to that reported before.(5,8,17) This increase in ejection fraction was driven by improvement of strain in the infarct and peri-infarct regions, and occurred despite low levels of CDC engraftment, documented by quantitative PCR. Based on the size of the infarct, we estimate that complete cellular replacement of the infarct zone would require >1 million cells. (18,19) Since the number of surviving CDCs is too low to provide direct contractile support via differentiation into cardiac myocytes, our results support the notion that paracrine mechanisms (7) play a major role in the functional benefits of CDC transplantation post-MI. Previous studies using CDCs reveal that these cells secrete an array of cytokines and growth factors, including IGF-1 (insulin-like growth factor-1), HGF (hepatocyte growth factor) and VEGF (vascular endothelial growth factor(20,21)) that have been shown to play a protective role post-MI, by reducing cell death, improving the microcirculation and attenuating adverse remodeling. (22-26) In addition to tissue preservation, paracrine factors can also influence viable infarct border-zone myocytes, promote recruitment of endogenous stem cells and boost the regenerative capacity of the heart post-infarct. (27) Histopathology studies in experimental models confirm that CDCs induce cardiac regeneration by direct (engrafting, differentiating into cardiac myocytes and endothelial cells) and paracrine mechanisms. (5,28,29)

The novel result of this study is that CDC transplantation resulted in improvement of LVEF and strain parameters of the infarct and peri-infarct zones at 4 weeks, but not 1 week following transplantation/infarction. This finding suggests that a *direct paracrine effect on contractility* of surviving myocytes in the infarct/peri-infarct region probably does not play a role in improving function, since maximum growth factor secretion by transplanted CDCs has been detected in the first week following transplantation.(7) Since measurements were

not performed immediately post-MI (due to technical reasons), we cannot rule out the possibility that the CDC-treated group had larger MIs at baseline, and CDC therapy influenced infarct size positively at 1week, resulting in lack of difference between the CDC and PBS groups. Nevertheless, the CDC-treated group continued to improve after 1 week, while the PBS-treated group worsened, suggesting that *cardiac regeneration* played a major role.

We used speckle tracking methodology for calculation of strain. The main advantage of this technique over tissue doppler imaging-based strain measurements (30),(31),(32) is that *1)* measurements are angle independent and *2)* it can distinguish active from passive movement. Strain-based parameters are sensitive indicators of regional and global cardiac function, and have been extensively validated in experimental and human studies. Ultrasound derived strain is an inexpensive and reliable means of quantifying the regional and global response to stem cell transplantation. In our study, we offer yet another potential application of strain in stem cell transplantation, namely, the assessment of dyssynchrony. The evolution of dyssynchrony after stem cell transplant appears to be concordant with improvement in function suggesting that improvements in dyssynchrony may be a potential mechanism by which stem cell transplantation improves regional and global function despite low engraftment rates.

## Study limitations

In the current study we used only circumferential strain measurements because we found that radial and longitudinal strains are unreliable in a small animal model. This study focused on evaluating the mechanical basis for changes in regional and global function after stem cell therapy. Accordingly, detailed analysis of potential molecular and cellular changes was not within the scope of the study. Additionally, we did not perform histopathology or test whether the effects of stem cell therapy are long lasting. But, based on previous detailed studies in CDCs that demonstrated regeneration of blood vessels and cardiac myocytes in the infarcted region (5,28), we would anticipate sustained functional benefit following CDC therapy. Here, we compared the effects of CDC therapy with PBS and did not include an additional control group like fibroblasts since previous studies by our group revealed that fibroblast transplantation did not result in paracrine factor secretion(29) or improvement in ejection fraction (5). Additionally, we did not have a sham group that would have evaluated the effects of injection on local tissue and angiogenic effects in normal myocardium. Lastly, since rodent infarctions are often very eccentric, the true volumes reported here may not be accurate, but we anticipate that this error would be equal for both groups.

## Conclusion

CDC transplantation following acute MI improved regional and global contractile function, and decreased dyssynchrony of the infarct/peri-infarct region, 4 weeks post-MI/ transplantation, despite low CDC engraftment. Based on these results, ongoing attempts to increase stem cell engraftment would be expected to decrease dyssynchrony even further by augmenting cardiac regeneration.

## Supplementary Material

Refer to Web version on PubMed Central for supplementary material.

## Acknowledgments

## Abbreviations and Acronyms

| | |
|---|---|
| **rCDC** | rat cardiosphere-derived stem cells |
| **CRT** | Cardiac resynchronization therapy |
| **$^{18}$FDG** | $^{18}$F-fluorodeoxyglucose |
| **CT** | Computed Tomography |
| **LVESV** | Left ventricular end systolic volume |
| **LVEDV** | Left ventricular end diastolic volume |
| **IMDM** | Iscove's Modified Dulbecco's Media |
| **PET** | Positron Emission Tomography |
| **PBS** | Phosphate Buffered Solution |
| **qPCR** | Quantitative, real time polymerase chain reaction |
| **WKY** | Wistar Kyoto |

## References

1. Gheorghiade M, Sopko G, De Luca L, Velazquez EJ, Parker JD, Binkley PF, et al. Navigating the crossroads of coronary artery disease and heart failure. Circulation. 2006; 114:1202–13. [PubMed: 16966596]

2. Moss AJ, Hall WJ, Cannom DS, Klein H, Brown MW, Daubert JP, et al. Cardiac-resynchronization therapy for the prevention of heart-failure events. N Engl J Med. 2009; 361:1329–38. [PubMed: 19723701]

3. Bleeker GB, Kaandorp TA, Lamb HJ, Boersma E, Steendijk P, de Roos A, et al. Effect of posterolateral scar tissue on clinical and echocardiographic improvement after cardiac resynchronization therapy. Circulation. 2006; 113:969–76. [PubMed: 16476852]

4. van Ramshorst J, Atsma DE, Beeres SL, Mollema SA, Marsan N Ajmone, Holman ER, et al. Effect of intramyocardial bone marrow cell injection on left ventricular dyssynchrony and global strain. Heart. 2009; 95:119–24. [PubMed: 18198204]

5. Smith RR, Barile L, Cho HC, Leppo MK, Hare JM, Messina E, et al. Regenerative potential of cardiosphere-derived cells expanded from percutaneous endomyocardial biopsy specimens. Circulation. 2007; 115:896–908. [PubMed: 17283259]

6. Johnston PV, Sasano T, Mills K, Evers R, Lee ST, Smith RR, et al. Engraftment, differentiation, and functional benefits of autologous cardiosphere-derived cells in porcine ischemic cardiomyopathy. Circulation. 2009; 120:1075–83. 7 p following 1083. [PubMed: 19738142]

7. Chimenti I, Smith RR, Li TS, Gerstenblith G, Messina E, Giacomello A, et al. Relative roles of direct regeneration versus paracrine effects of human cardiosphere-derived cells transplanted into infarcted mice. Circ Res. 106:971–80. [PubMed: 20110532]

8. Davis DR, Kizana E, Terrovitis J, Barth AS, Zhang Y, Smith RR, et al. Isolation and expansion of functionally-competent cardiac progenitor cells directly from heart biopsies. J Mol Cell Cardiol. 2010; 49:312–21. [PubMed: 20211627]

9. Pouzet B, Vilquin JT, Hagege AA, Scorsin M, Messas E, Fiszman M, et al. Intramyocardial transplantation of autologous myoblasts: can tissue processing be optimized? Circulation. 2000; 102:III210–5. [PubMed: 11082389]

10. Helm RH, Leclercq C, Faris OP, Ozturk C, McVeigh E, Lardo AC, et al. Cardiac dyssynchrony analysis using circumferential versus longitudinal strain: implications for assessing cardiac resynchronization. Circulation. 2005; 111:2760–7. [PubMed: 15911694]

11. Langeland S, D′Hooge J, Wouters PF, Leather HA, Claus P, Bijnens B, et al. Experimental validation of a new ultrasound method for the simultaneous assessment of radial and longitudinal myocardial deformation independent of insonation angle. Circulation. 2005; 112:2157–62. [PubMed: 16203928]

12. Fukushima S, Varela-Carver A, Coppen SR, Yamahara K, Felkin LE, Lee J, et al. Direct intramyocardial but not intracoronary injection of bone marrow cells induces ventricular arrhythmias in a rat chronic ischemic heart failure model. Circulation. 2007; 115:2254–61. [PubMed: 17438152]

13. Koopman LP, Slorach C, Hui W, Manlhiot C, McCrindle BW, Friedberg MK, et al. Comparison between different speckle tracking and color tissue Doppler techniques to measure global and regional myocardial deformation in children. J Am Soc Echocardiogr. 2010; 23:919–28. [PubMed: 20655173]

14. Das H, George JC, Joseph M, Das M, Abdulhameed N, Blitz A, et al. Stem cell therapy with overexpressed VEGF and PDGF genes improves cardiac function in a rat infarct model. PLoS One. 2009; 4:e7325. [PubMed: 19809493]

15. Cohn JN, Ferrari R, Sharpe N. Cardiac remodeling--concepts and clinical implications: a consensus paper from an international forum on cardiac remodeling. Behalf of an International Forum on Cardiac Remodeling. J Am Coll Cardiol. 2000; 35:569–82. [PubMed: 10716457]

16. Mewton N, Croisille P, Revel D, Weber O, Higgins CB, Saeed M. Left ventricular postmyocardial infarction remodeling studied by combining MR-tagging with delayed MR contrast enhancement. Invest Radiol. 2008; 43:219–28. [PubMed: 18340245]

17. Terrovitis J, Lautamaki R, Bonios M, Fox J, Engles JM, Yu J, et al. Noninvasive quantification and optimization of acute cell retention by in vivo positron emission tomography after intramyocardial cardiac-derived stem cell delivery. J Am Coll Cardiol. 2009; 54:1619–26. [PubMed: 19833262]

18. Olivetti G, Capasso JM, Sonnenblick EH, Anversa P. Side-to-side slippage of myocytes participates in ventricular wall remodeling acutely after myocardial infarction in rats. Circ Res. 1990; 67:23–34. [PubMed: 2364493]

19. Caulfield JB, Leinbach R, Gold H. The relationship of myocardial infarct size and prognosis. Circulation. 1976; 53:I141–4. [PubMed: 1253347]

20. Chimenti ISR, Leppo M, Gerstenblith G, Giacomello A. Secretion of pro-survival and pro-angiogenic growth factors in vitro and in vivo by cardiac progenitor cells from human biopsies. Circ Res. 2007; 101

21. Stastna M, Chimenti I, Marban E, Van Eyk JE. Identification and functionality of proteomes secreted by rat cardiac stem cells and neonatal cardiomyocytes. Proteomics. 2010; 10:245–53. [PubMed: 20014349]

22. Hausenloy DJ, Yellon DM. Cardioprotective growth factors. Cardiovasc Res. 2009; 83:179–94. [PubMed: 19218286]

23. Davis ME, Hsieh PC, Takahashi T, Song Q, Zhang S, Kamm RD, et al. Local myocardial insulin-like growth factor 1 (IGF-1) delivery with biotinylated peptide nanofibers improves cell therapy for myocardial infarction. Proc Natl Acad Sci U S A. 2006; 103:8155–60. [PubMed: 16698918]

24. Jin H, Wyss JM, Yang R, Schwall R. The therapeutic potential of hepatocyte growth factor for myocardial infarction and heart failure. Curr Pharm Des. 2004; 10:2525–33. [PubMed: 15320761]

25. Ueda H, Nakamura T, Matsumoto K, Sawa Y, Matsuda H. A potential cardioprotective role of hepatocyte growth factor in myocardial infarction in rats. Cardiovasc Res. 2001; 51:41–50. [PubMed: 11399246]

26. Li Q, Li B, Wang X, Leri A, Jana KP, Liu Y, et al. Overexpression of insulin-like growth factor-1 in mice protects from myocyte death after infarction, attenuating ventricular dilation, wall stress, and cardiac hypertrophy. J Clin Invest. 1997; 100:1991–9. [PubMed: 9329962]

27. Rota M, Padin-Iruegas ME, Misao Y, De Angelis A, Maestroni S, Ferreira-Martins J, et al. Local activation or implantation of cardiac progenitor cells rescues scarred infarcted myocardium improving cardiac function. Circ Res. 2008; 103:107–16. [PubMed: 18556576]

28. Messina E, De Angelis L, Frati G, Morrone S, Chimenti S, Fiordaliso F, et al. Isolation and expansion of adult cardiac stem cells from human and murine heart. Circ Res. 2004; 95:911–21. [PubMed: 15472116]

29. Chimenti I, Smith RR, Li TS, Gerstenblith G, Messina E, Giacomello A, et al. Relative roles of direct regeneration versus paracrine effects of human cardiosphere-derived cells transplanted into infarcted mice. Circ Res. 2010; 106:971–80. [PubMed: 20110532]

30. Reisner SA, Lysyansky P, Agmon Y, Mutlak D, Lessick J, Friedman Z. Global longitudinal strain: a novel index of left ventricular systolic function. J Am Soc Echocardiogr. 2004; 17:630–3. [PubMed: 15163933]

31. D′Hooge J, Konofagou E, Jamal F, Heimdal A, Barrios L, Bijnens B, et al. Two-dimensional ultrasonic strain rate measurement of the human heart in vivo. IEEE Trans Ultrason Ferroelectr Freq Control. 2002; 49:281–6. [PubMed: 11885685]

32. Leitman M, Lysyansky P, Sidenko S, Shir V, Peleg E, Binenbaum M, et al. Two-dimensional strain-a novel software for real-time quantitative echocardiographic assessment of myocardial function. J Am Soc Echocardiogr. 2004; 17:1021–9. [PubMed: 15452466]
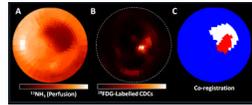
**Figure 1. In vivo PET imaging**

CDCs were identified in the infarct region and border-zone, 1 hour following intra-myocardial injection. Polarmap presentation of $^{13}$NH$_3$ perfusion PET (A) and $^{18}$FDG-labeled CDCs PET (B) from the same 3D sampling points.

C. Co-registered polar map of perfusion defect (white) and CDCs signal (red). Regions were defined using 60% threshold from maximum counts. Transplanted CDCs signal is found mainly in the region of the perfusion defect.
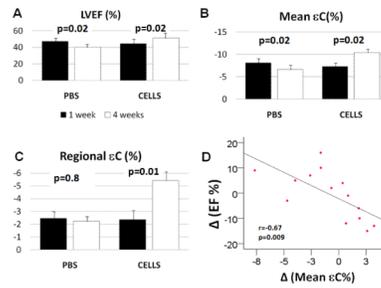
**Figure 2. CDC transplantation improved function of infarcted region**

A. Ejection fraction significantly improved in CDC-treated animals, but decreased in PBS-treated animals at 4 weeks following MI.

B. Mean circumferential strain of the apex improved significantly in the CELL group and worsened in the PBS group 4 weeks following MI.

C. Regional circumferential strain of the infarcted region (apex) improved in CDC-treated animals, 4 weeks post-MI/cell transplantation.

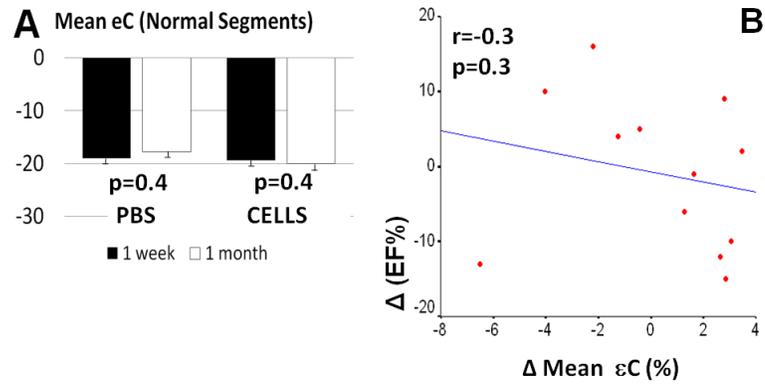D. Improvement in mean circumferential strain of the apex was correlated with improvement in global LVEF.

**Figure 3. CDC transplantation had no effect on function of remote, non-infarcted region**
A. Circumferential strain in non-infarcted (basal) segments did not change significantly at 4 weeks post-MI and was not correlated with change in LVEF (B).
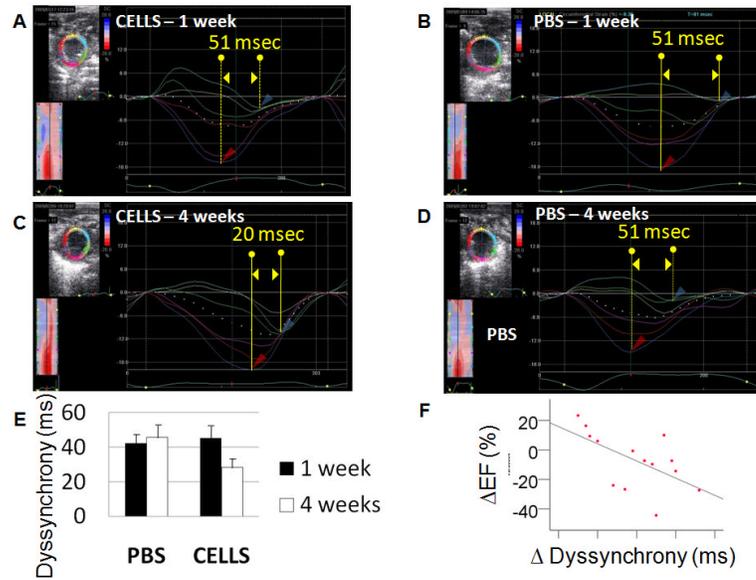
**Figure 4. CDC transplantation decreased dyssynchrony of infarcted region**
Representative 2-D circumferential strain images of the apical short-axis views in a CELL-treated (A) and PBS-treated (B) animal.

C. Dyssynchrony in the infarct/peri-infarct region was decreased in CDC- treated animals but was unchanged in PBS-treated animals.

D. Increase in LVEF correlated with decrease in dyssynchrony of infarct/peri-infarct region, 4 weeks post-MI.

**Table 1**

Echocardiography parameters of non-infarcted animals (n=10)

| | Base | Apex | P |
|---|---|---|---|
| **Mean Circumferential Strain (%)** | −22.6±3.1 | −23.0±5.7 | 0.866 |
| **Mechanical Delay (msec)** | 12.1±5.6 | 9.4±2.5 | 0.244 |
| **Heart rate (b/min)** | 283±43 | | |
| **Ejection fraction (%)** | 76.2±6.7 | | |
| **LVEDV (uL)** | 189±65 | | |
| **LVESV (uL)** | 44±19 | | |